Modelling and Implementation of Multi-source Isolated Microgrid Using Virtual Synchronous Generator Technology

CHEN Xing[1], *QIAN Shengnan*[2], *LI Fei*[1], *GE Zhaohui*[1], *CAO Xin*[2*]

1. China Construction Power and Environment Engineering Co. Ltd., Nanjing 211100, P.R.China;
2. College of Automation Engineering, Nanjing University of Aeronautics and Astronautics, Nanjing 211106, P.R.China

(Received 15 July 2021; revised 10 August 2021; accepted 15 September 2021)

Abstract: To improve the living standards, economical efficiency and environmental protection of isolated islands, remote areas and other areas with weak electric power facilities construction, a multi-source independent microgrid system is studied, including diesel generators, photovoltaic power generation system, wind power generation system and energy storage unit. Meanwhile, in order to realize the voltage and frequency stability control of AC bus of multi-source microgrid, the virtual synchronous generator technology is introduced into the energy storage unit, and the charge and discharge control of the energy storage battery are simulated as the control behavior characteristics of synchronous motors, so as to provide damping and inertia support for the microgrid. The operation mode and control principle of each energy subsystem are expounded and analyzed. The algorithm principle of virtual synchronous generator and the control method of energy storage unit are given. Then, the working modes of the microgrid system under different environmental conditions are analyzed, and the multi-source microgrid system simulation model is built based on MATLAB /Simulink. The simulation results show that the microgrid system can run stably under different working modes and the energy storage unit using the virtual synchronous generator technology can provide good voltage and frequency support for the microgrid system. Finally, experiments verify the supporting function of energy storage unit on the voltage and frequency of the microgrid system.

Key words: isolated microgrid; wind/solar/diesel/storage; virtual synchronous generator; modelling

CLC number: TM727 **Document code:** A **Article ID:** 1005-1120(2021)05-0747-11

0 Introduction

With the rapid development of technology and economy, the level of electrification in China is continuously improving, but there are still tens of millions of people without electricity in remote mountainous areas or islands. At the same time, China has a large number of overseas construction projects along the overseas "the Belt and Road" route, and there may be negative factors, such as weak power grid capacity, high oil price cost, or even double disconnection of oil and electricity, which put great pressure on the duration of the project. These areas have the disadvantages of long transmission distance and high cost of grid extension, so it is necessary to make use of renewable energy according to local conditions and establish independent microgrid system[1].

Microgrid is a power system composed of distributed energy and load, which is an independent controlled unit relative to the large power grid, and can be operated in grid-connected or independent mode[2]. However, due to the lack of large power grid support, the main power source is needed to provide stable voltage and frequency. The renewable energy (solar energy, wind energy, etc.) in the microgrid is influenced by environmental factors, and the output power is intermittent and random, which causes instantaneous power fluctuation

*Corresponding author, E-mail address: caoxin@nuaa.edu.cn.

How to cite this article: CHEN Xing, QIAN Shengnan, LI Fei, et al. Modelling and implementation of multi-source isolated microgrid using virtual synchronous generator technology[J]. Transactions of Nanjing University of Aeronautics and Astronautics, 2021, 38(5): 747-757.

http://dx.doi.org/10.16356/j.1005-1120.2021.05.004

in the operation of the microgrid system[3-4]. Therefore, in addition to the main power source, the energy storage unit is usually required to realize the fast response to instantaneous power fluctuation and power peak shaving and valley filling[5].

In recent years, a number of independent microgrid demonstration projects have been built at home and abroad[6-8]. The EU-led More Microgrids Project builds small-capacity microgrids through photovoltaic systems and batteries on the Greek Island of Kythnos, while Japan has built independent microgrid demonstration projects on dozens of islands. In 2009, China's first independent renewable energy power station was built in Dangan Island, Zhuhai, to provide domestic and desalination electricity using solar, wind and wave energy. In 2011, an independent microgrid system designed by Zhejiang Electric Power Research Institute was put into use in Dongfushan Island, Zhejiang Province, with the optimization goal of maximizing energy utilization and battery life. Many achievements have also been made in the theoretical research of independent microgrid system. Ref.[9] established a wind-solar storage microgrid system to realize seamless switching of off-grid operation, but did not give specific modelling methods for each module. Ref.[10] established the wind-solar-diesel storage microgrid system, gave the modelling process of each module, and verified the anti-interference ability of the system through simulation, but did not consider the different working modes of the system. Ref.[11] studied the coordinated control between diesel engine and energy storage system, and introduced droop control into the energy storage system to alleviate the long-term overcurrent problem of diesel engine. However, distributed power sources in the above mentioned literatures are all conventional grid-connected converters, lacking inertia and damping, and unable to provide excellent voltage and frequency support for microgrid systems.

The power electronic interface of conventional grid-connected converter weakens the inertia and damping characteristics of microgrid and brings stability problems[12]. Therefore, some scholars put forward the concept of virtual synchronous generator (VSG)[13], which makes the converter simulate the inertia, primary frequency modulation and voltage regulation characteristics of synchronous motors. At present, VSG technology is mainly divided into current control type and voltage control type[14]. Compared with current-controlled VSG, voltage-controlled VSG is more suitable for distributed weak grid environment with high energy permeability[15]. Refs.[16-17] analyzed and verified the supporting effect of VSG strategy on the stability of microgrid. Ref.[18] introduced VSG technology into the charging pile of microgrid to make electric vehicles participate in primary and secondary frequency modulation and improve the dynamic performance of microgrid.

In this context, this paper establishes an independent multi-source microgrid system, including diesel engine, photovoltaic power generation system, wind power generation system, energy storage unit and load system. Among them, the output power of photovoltaic system and wind power generation system is greatly affected by the environment, and the battery as the main power source needs large capacity, so diesel engine is chosen as the main power source to provide stable voltage and frequency for the system. In the microgrid system, the photovoltaic array of 30 kW is used in the photovoltaic system, the doubly-fed induction machine is used in the wind power system, the storage battery is used in the energy storage unit, VSG technology is introduced into the front bi-directional AC/DC converter, and the voltage-controlled synchronverter scheme[15] is adopted, which can comprehensively simulate the electromagnetic characteristics, rotor inertia, frequency regulation and voltage regulation characteristics of the synchronous motor. The main load characteristics are also taken into account in the load system. In this paper, each subsystem of the microgrid is theoretically studied, and the MATLAB/Simulink simulation model is established. At the same time, the simulation verification is carried out according to different operation modes of the independent microgrid, and the response and support performance of the energy storage unit to the voltage and frequency of the microgrid system is verified by experimental results.

1 Microgrid System Architecture

The microgrid system studied in this paper is an AC independent microgrid system, which does not participate in grid connection. The microgrid system makes full use of local renewable energy and establishes multiple power modules to cooperate with each other to realize the stable operation of the microgrid. The structure of the microgrid system is shown in Fig. 1. The main modules include diesel power generation system, photovoltaic power generation system, wind power generation system, energy storage unit and load system. Diesel generator system is the main power source, which provides stable voltage and frequency for the microgrid system. Photovoltaic power generation system and wind power generation system are operated under the maximum power point tracking (MPPT) mode. The energy storage unit stores electricity when renewable energy sources are abundant and provides power to the microgrid system when renewable energy sources are scarce. The load system is composed of active and reactive loads.

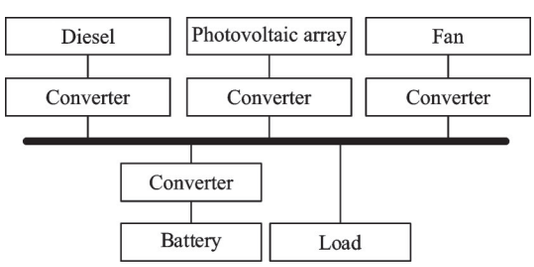

Fig.1 Structure of microgrid system

1.1 Diesel power generation system

Diesel power generation system operates as the main power source, balancing power supply and load consumption, and outputting 380 V/50 Hz AC power. Fig. 2 shows the control diagram of the diesel generator system, where f_{ref} and f are the grid frequency reference and actual grid frequency, and V_{ref} and V the grid voltage reference and actual grid voltage. The system consists of a diesel engine, a governor, a synchronous generator and an excitation regulator. The governor detects the frequency signal, adjusts the output power of the synchronous generator by controlling the output torque of the diesel engine, and realizes the frequency regulation. The excitation regulator detects the voltage signal and keeps the voltage amplitude of the microgrid stable by regulating the excitation voltage of the synchronous generator. Diesel power generation system maintains the quality of microgrid AC bus voltage by closed-loop control of voltage frequency and amplitude.

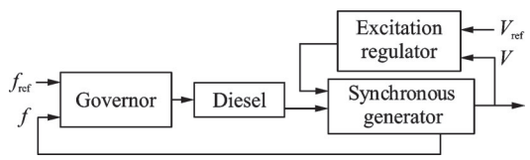

Fig.2 Control diagram of diesel power generation system

Fig. 3 shows the mathematical model of diesel engine speed regulation system, where ω_{ref} and ω are the speed reference and actual speed, respectively. T_m is the mechanical torque. T_1, T_2 and T_3 are the time constants of the controller. k is the proportional parameter of governor. T_4, T_5 and T_6 are the time constants of accelerator actuator. T_d is the engine lag time.

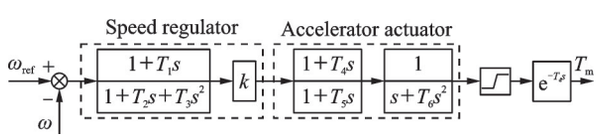

Fig.3 Mathematical model of diesel engine speed regulation system

Fig.4 shows the mathematical model of excitation regulation system. In Fig.4, U_{ref}, U and U_f are the voltage reference, the actual voltage and the excitation voltage, respectively. T_a and T_b are the time constants of the phase compensator. k_e, T_e, k_f and T_f are the proportional parameter of excitation regulator, the time constant of the excitation regulator, the differential parameter of the excitation stabilizer and the time constant of excitation stabilizer, respectively.

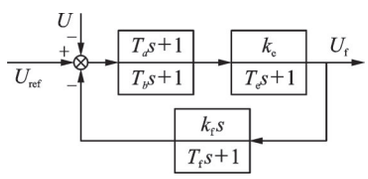

Fig.4 Mathematical model of excitation regulation system

1.2 Photovoltaic power generation system

The photovoltaic power generation system converts solar radiant energy into electrical energy under the photovoltaic effect. The output power of photovoltaic cells is non-linear under the influence of light intensity, junction temperature and load. The P-V curve has the maximum power point, and MPPT is used to improve the generation efficiency. As shown in Fig.5, the photovoltaic power generation system adopts a two-stage topology, where U_{pv}, I_{pv}, U_{dc}, U_g and I_g are the terminal voltage of the photovoltaic array, the output current of photovoltaic array, the DC side voltage of the inverter, the AC bus voltage and the grid-connected current, respectively.

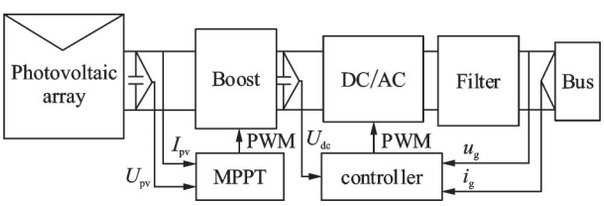

Fig.5 Structure of two-stage photovoltaic power generation system

The front-stage boost circuit increases the terminal voltage of the photovoltaic array, and MPPT is used to control the output power. MPPT control adopts disturbance observation method to detect the change of output voltage and current of photovoltaic array in real time and adjust the duty ratio of driving signal.

The DC/AC stage realizes grid-connected control, the DC into alternating current, through the filter circuit access to the AC bus. The mathematical model of inverter in the dq coordinate system is

$$\begin{cases} L\dfrac{\mathrm{d}i_d}{\mathrm{d}t} = u_d - e_d - Ri_d + \omega Li_q \\ L\dfrac{\mathrm{d}i_q}{\mathrm{d}t} = u_q - e_q - Ri_q + \omega Li_d \end{cases} \tag{1}$$

The voltage and current double closed-loop decoupling control diagram is shown in Fig.6, where V_{dc}^* and V_{dc} are the DC voltage reference and actual DC voltage. i_q^* and i_q are the q-axis current reference and actual q-axis current. i_d^* and i_d are the d-axis current reference and actual d-axis current. e_q and e_d are the feedforward q-axis voltage and d-axis voltage. v_q and v_d are the q-axis and the d-axis voltages of inverters. K_{uI} and K_{uP} are the proportional and integral parameters of the voltage loop. K_{iI} and K_{iP} are the proportional and integral parameters of the current loop.

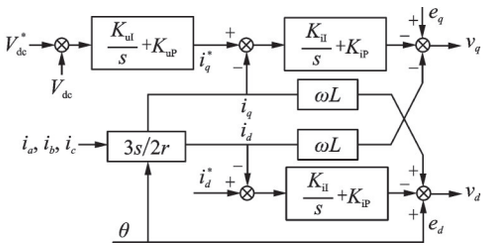

Fig.6 Control diagram of double closed-loop decoupling of inverters

1.3 Wind power generation system

The wind energy is utilized to drive the blades of the wind turbine to rotate to generate mechanical energy, which drives the doubly-fed induction generator (DFIG) to rotate. The gearbox regulates the speed of the wind turbine and DFIG, and the mechanical energy is converted into electrical energy output through DFIG. The AC excitation converter consists of two back-to-back PWM converters, and the grid-side converter adopts voltage and current double closed-loop control. The wind power generation system is shown in Fig.7. In Fig.7, n_w and n_r denote the speeds of fan and DFIG. P_{wind} is the mechanical energy generated by the fan. P_s and Q_s are the active and reactive power outputs of the DFIG stator. f_1 and f_r are the frequencies of microgrid and DFIG. P_r and Q_r are the active and reactive powers absorbed by the DFIG rotor. P_g and Q_g are the active and reactive power inputs of the microgrid.

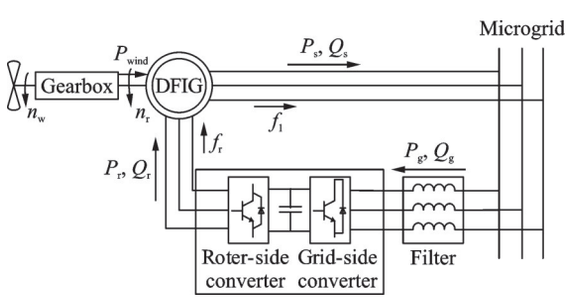

Fig.7 Structure block of doubly fed wind power generation system

The mechanical power of the wind turbine is

$$P_{\text{wind}} = \frac{1}{2} C_p(\beta,\lambda)\rho\pi R^2 V_\omega^3 \tag{2}$$

where ρ, R, λ, β, ω, $C_p(\beta,\lambda)$, V_ω are the air density, the fan radius, the blade tip speed ratio, the pitch angle, the wind wheel speed, the wind energy utilization coefficient, and the air velocity, respectively. The active power and reactive power emitted by the stator are

$$\begin{cases} P_s = \dfrac{3}{2}\dfrac{L_m}{L_s} U_s i_{rd} \\ Q_s = -\dfrac{3}{2}\left(\dfrac{L_m}{L_s} U_s i_{rq} + \dfrac{U_s^2}{L_s \omega_1}\right) \end{cases} \tag{3}$$

where L_m denotes the mutual inductance in stator winding, L_s the inductance of the stator winding, U_s the microgrid voltage, and ω_1 the frequency of microgrid. i_{rd} and i_{rq} are the d-axis current and q-axis current at the rotor side.

1.4 Load system

In recent years, permanent magnet synchronous motor (PMSM) has been widely used in industry such as pumps and fans, which has the advantages of soft start, smooth speed regulation and low harmonic pollution. The motor load system is established to simulate the characteristics of the main power load in the microgrid system. Fig.8 is the control diagram of the permanent magnet motor servo speed regulating system, which adopts double closed-loop control of speed and current. In Fig.8, i_a, i_b and i_c are the three-phase currents, n_{ref} and n the motor speed reference and actual speed, $i_{q\text{ref}}$ and $i_{d\text{ref}}$ the q-axis current reference and d-axis current reference, u_q and u_d the q-axis and the d-axis voltages of inverters, and s_a, s_b and s_c the drive signals. Space vector pulse width modulation (SVM) is adopted in the system.

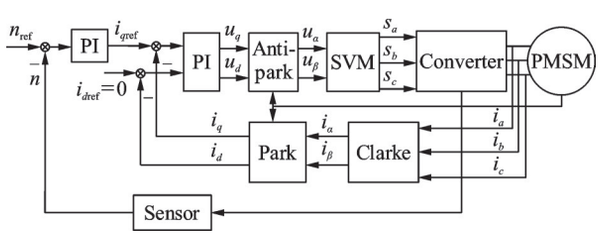

Fig.8 Control block of permanent magnet motor servo speed control system

In general, for ideal pump type load, the load torque and speed are quadratic. However, the pump works in a liquid environment actually, so in the starting process and low speed operation, it needs to overcome great fluid resistance. In addition, it also needs to overcome certain resistance in stable operation. The relationship between load torque T_L and speed n is about 1.5 power function in stable operation. Its load torque characteristics are shown in Fig.9.

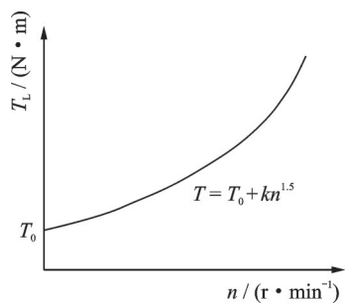

Fig.9 Load torque characteristic curve of electric pump

In the simulation modelling analysis, the resistive load and series RLC load are used to represent the active and reactive loads, respectively, for other equipment.

2 Energy Storage Unit with VSG Technology

When the unbalance between the supply and demand of active and reactive power in the microgrid system causes frequency and voltage offset rating problems, the energy storage unit can play an important role in suppressing the power fluctuation. The energy storage unit adopts a two-stage structure, and the front stage is connected to the grid through a full bridge converter. Because the rated voltage of the battery is low, the three-phase PWM rectifier is a Boost-type converter. Charging needs Buck converter for power conversion, discharge with Boost for power conversion. Therefore, the post-stage adopts Buck/Boost bi-directional converter to connect the battery. Fig.10 shows the circuit topology of the energy storage unit. v_a, v_b, v_c are three-phase voltages of the microgrid. L_S and R_S are

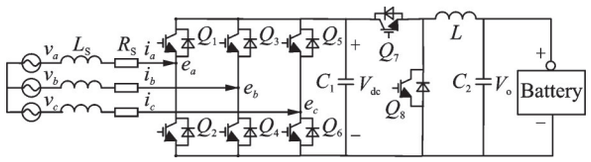

Fig.10 Topology of energy storage unit

the inductors and additional resistors of grid-connected filtering, respectively. Q_1—Q_6 are full bridge circuit switches. Q_7 and Q_8 are post-stage DC/DC circuit switches. C_1 and C_2 are the voltage stabilizing capacitances.

In order to make the energy storage module have inertia and damping to support the microgrid, the VSG algorithm is adopted in the front stage bidirectional AC/DC converter. VSG algorithm introduces the synchronous generator mathematical model into the converter control algorithm, which can simulate the frequency and voltage regulation characteristics of the synchronous motor.

The control block diagram is shown in Fig.11. In the two-stage structure of the energy storage unit, the DC side voltage is stabilized by the front stage, and the primary voltage regulation function is realized. i is the AC input current. v is the voltage of microgrid. V_{dcref} and V_{dc} are the reference and actual values of the DC voltage. T_{m} is the virtual mechanical torque. T_{e} is the virtual electromagnetic torque. J is the virtual moment of inertia. D_{p} is virtual damping coefficient. Q_{ref} and Q are the reference and actual value of reactive power respectively. K is the reactive power regulation coefficient. $M_{\mathrm{f}}i_{\mathrm{f}}$ is the virtual excitation parameter. v_{ref} is the reference value of the effective value of the microgrid voltage. K_{v} is the

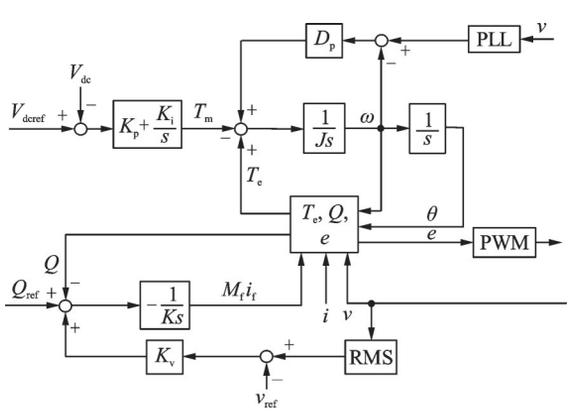

Fig.11 Control diagram of VSG algorithm

voltage-reactive power regulation factor. K_{p} and K_{i} are the proportional and integral parameters of the voltage loop. PWM denotes pulse-width modulation. RMS denotes root mean square. PLL denotes phase locked loop. The VSG algorithm is

$$\begin{cases} J\dfrac{\mathrm{d}^2\theta}{\mathrm{d}t^2}=T_{\mathrm{e}}-T_{\mathrm{m}}-D_{\mathrm{p}}\dfrac{\mathrm{d}\theta}{\mathrm{d}t} \\ \dfrac{-1}{Ks}\left[Q_{\mathrm{ref}}-Q+K_{\mathrm{v}}(v-v_{\mathrm{ref}})\right]=M_{\mathrm{f}}i_{\mathrm{f}} \end{cases} \tag{4}$$

The primary frequency regulation is introduced into the post-stage bidirectional DC/DC converter to support the active power of the microgrid. The battery can be charged and discharged with constant current or constant power according to different needs. Charging current in constant current mode is set as

$$I_{\mathrm{L}}^{*}=I_{\mathrm{Lref}}+\left(K_{\mathrm{f}}+\frac{K_{\mathrm{fi}}}{s}\right)(f_{\mathrm{g}}-f_{\mathrm{r}}) \tag{5}$$

where I_{L}^{*} is the given value of charging current, I_{Lref} the charging current reference value, f_{r} the microgrid frequency reference, and f_{g} the microgrid frequency. K_{f} and K_{fi} are the frequency modulation proportional and integral parameters of the energy storage unit. When the integral parameter is introduced to make the total output power of the power supply fail to meet the load demand, the energy storage unit can provide more power.

3 Working State and Simulation Analysis of Independent Microgrid System

Based on the MATLAB/Simulink platform, a model of the microgrid system is built, as shown in Fig.12, to verify the stable operation of the microgrid system under different modes. The system

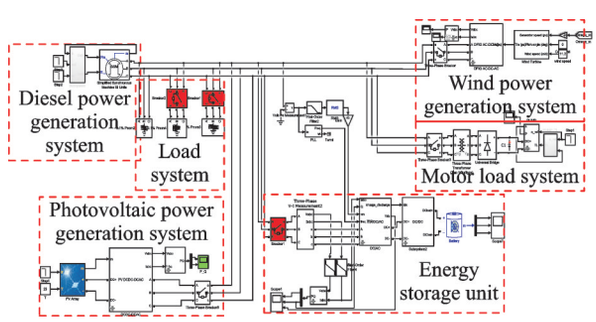

Fig.12 Simulation model of microgrid system

works in different modes under different natural environment and battery state of charge.

3.1 Mode 1

When the intensity of wind and light is weak and the renewable energy generation system almost provides no electric energy, the electric energy required by microgrid is provided by the diesel engine generation system and energy storage unit, and the battery works in the discharge mode. If the battery state of charge(SOC) reaches the lower limit, SOC$<$ SOC_{min}, the battery cannot discharge and only the diesel engine supplies electricity at this time.

Initially, the diesel engine runs with an active load of 30 kW. When t=5 s, the active load increases by 10 kW, and the microgrid frequency drops. Fig. 13 shows the frequency and voltage magnitude waveform of the microgrid. After a sudden load increase, the frequency immediately drops to about 0.15 Hz, and then returns to 50 Hz after about 5 s. When t=10 s, the inductive reactive power load of 10 kW is increased to simulate the voltage drop of microgrid. After the sudden increase of reactive load, the voltage drops instantly about 2.5 V, and the voltage recovers after about 2 s.

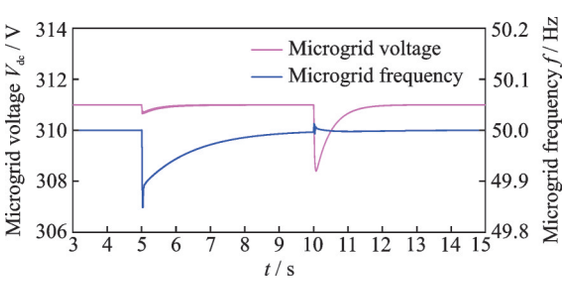

Fig.13 Waveform of microgrid voltage magnitude and frequency under Mode 1

3.2 Mode 2

When the renewable energy is sufficient and the total electric energy provided is higher than the load demand, there will be surplus system energy in addition to the supply to the load. If the battery is not fully charged, i.e. SOC $<$ SOC_{max}, the energy storage unit works under the charging mode and transmits part of the electric energy to the battery for storage. If the battery has reached the maximum state of charge, the energy storage unit does not work. At the same time, the photovoltaic power generation system or wind power generation system should be changed from the MPPT mode to the constant power mode.

To verify the supporting effect of energy storage unit on the voltage and frequency of the microgrid, the diesel engine was set to work in the open-loop mode with the rated output power of 40 kW. The wind power system and photovoltaic power system both output power 30 kW. The energy storage unit works under the charging mode, and the charging power is 20 kW. Meanwhile, 80 kW active load is connected as well.

When t=1 s, the system runs steadily. Due to the open-loop operation of the diesel engine, the inductance in the line and the coil in the motor, the actual load is inductive and the voltage is lower than the rated value. When t=1.5 s, the energy storage unit enables droop algorithm. The reactive power output of the energy storage unit makes up for the perceptual reactive power missing in part of the system, and the voltage amplitude of the microgrid rises. At t=2.5 s, 10 kW active load is removed to simulate the frequency drop of the microgrid. At this point, the frequency-active droop algorithm of the energy storage unit responds, and the battery reduces its own charging power to compensate the required active power. As shown in Fig. 14, the microgrid frequency gradually rises under the action of droop algorithm. The output active power and reactive power of the energy storage unit are shown in Fig. 15. The current waveforms of the energy storage unit are shown in Figs.16, 17. The current changes smoothly with the drooping instruction.

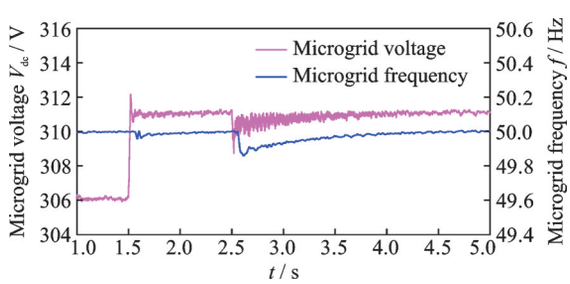

Fig.14 Waveform of microgrid voltage magnitude and frequency under Mode 2

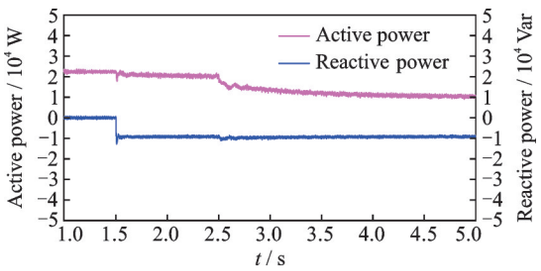

Fig.15 Waveform of active power and reactive power of energy storage unit under Mode 2

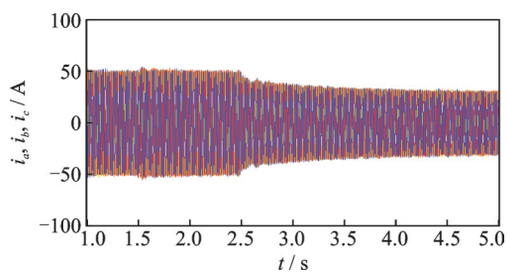

Fig.16 Current waveform of energy storage unit under Mode 2

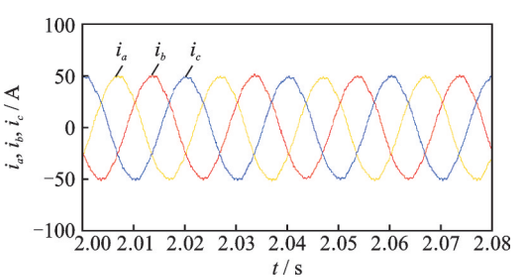

Fig.17 Enlarged current waveform of energy storage unit under Mode 2

3.3 Mode 3

When the total electric energy provided by renewable energy and diesel engine does not meet the load demand, if the battery SOC $>$ SOC_{min}, the energy storage unit works in the discharge mode. If SOC $<$ SOC_{min}, the battery does not support discharge. To maintain the normal operation of the microgrid, the secondary load needs to be removed.

The diesel engine is set to work in open loop-mode and the rated output power is 40 kW. Wind power system and photovoltaic power system output 30 kW power, respectively. The energy storage unit works in the discharge mode, and the discharge power is 20 kW, in which 120 kW active load is connected.

When t =1 s, the system runs steadily. When t=1.5 s, the energy storage unit enables droop algorithm. The reactive power output of the energy storage unit makes up for the perceptual reactive power missing in part of the system. As shown in Fig.18, the voltage amplitude of the microgrid rises. When t=2.5 s, 10 kW active load is removed to simulate the frequency drop of the microgrid. At this point, the frequency-active droop algorithm of the energy storage unit responds, and the battery increases the discharge power to compensate the required active power. As shown in Fig.18, the microgrid frequency gradually rises under the action of droop algorithm. The output active power and reactive power of the energy storage unit are shown in Fig.19. The output current waveform of the energy storage unit is shown in Fig.20. The current changes smoothly with the droop instruction.

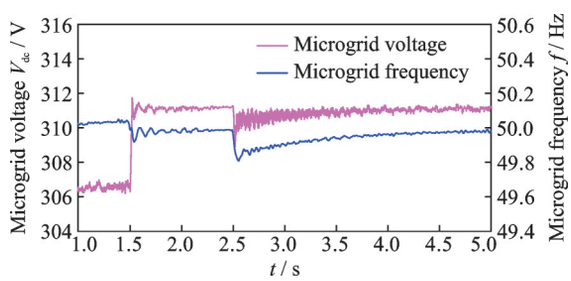

Fig.18 Waveform of microgrid voltage magnitude and frequency under Mode 3

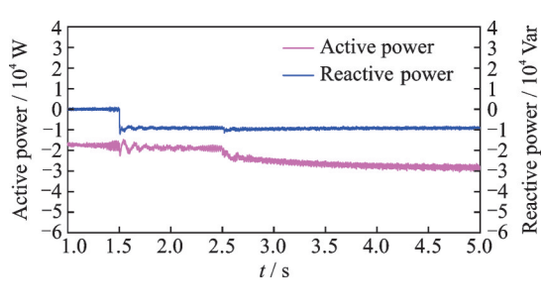

Fig.19 Waveform of active power and reactive power of energy storage unit under Mode 3

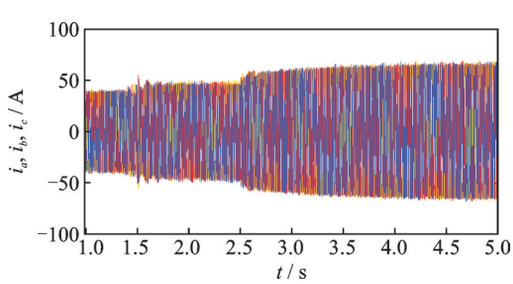

Fig.20 Waveform of current of energy storage unit under Mode 3

4 Experimental Results

In order to verify the response and support function of the energy storage unit using virtual synchronous generator technology to the frequency and voltage of microgrid, experiments are carried out by using CHROMA programmable three-phase AC power supply and a virtual synchronous rectifier. Limited by the power supply, the input AC voltage is 110 V, the energy storage unit works in the charging mode, and the steady-state power is 5 kW.

In order to verify the response and support function of the active power-frequency droop algorithm of the energy storage unit to the voltage frequency of the microgrid, the step value of voltage frequency is 0.25 Hz, and the sudden change of active power of energy storage unit with voltage frequency is 2.5 kW. As shown in Fig.21, the active power and current can change rapidly and steadily with the change of the microgrid frequency, and the frequency of the energy storage unit can quickly track the change. As shown in Figs. 22, 23, when the power grid frequency increases from 49.75 Hz to 50.25 Hz and decreases from 50.25 Hz to 49.75 Hz, the active power can respond quickly and takes about 80 ms. In order to verify the response and support function of the reactive power-voltage droop algorithm of the energy storage unit to the microgrid voltage, the step change of the microgrid voltage is set to 11 V(110 V×10%), and the reactive power output is 0 kVar. The sudden change value of the reactive power of the energy storage unit with the voltage is 5 kVar. As shown in Fig.24, when the microgrid voltage rises to 121 V, the energy storage unit emits capacitive reactive power 5 kVar. As shown in Fig.25, when the voltage drops to 99 V, the energy storage unit emits inductive reactive power 5 kVar. Reactive power can change rapidly with the change of microgrid voltage. In the process of voltage and reactive power change, the active power and the frequency of the energy storage unit return to the initial value after a small fluctuation, which remains basically unchanged.

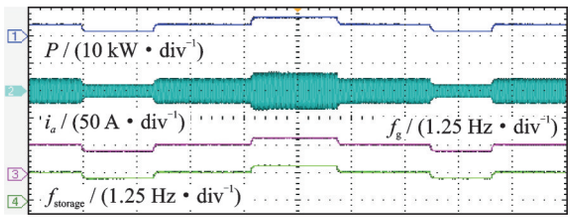

Fig.21 Experimental result when microgrid frequency step changes

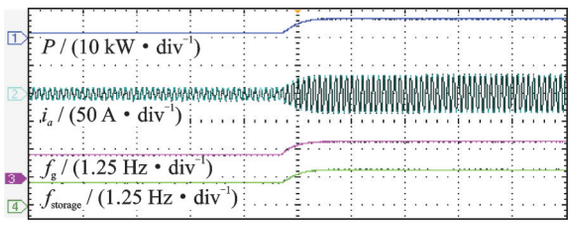

Fig.22 Experimental results when microgrid frequency step changes from 49.75 Hz to 50.25 Hz

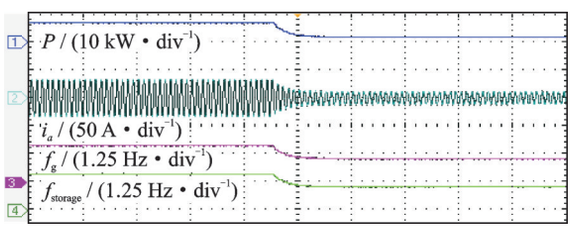

Fig.23 Experimental results when microgrid frequency step changes from 50.25 Hz to 49.75 Hz

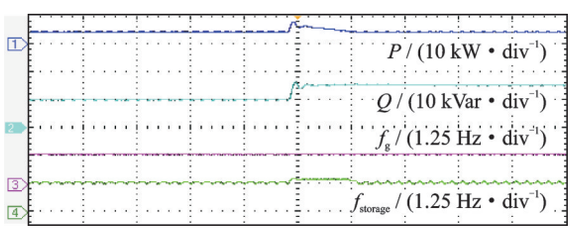

Fig.24 Experimental results when microgrid voltage step changes from 110 V to 121 V

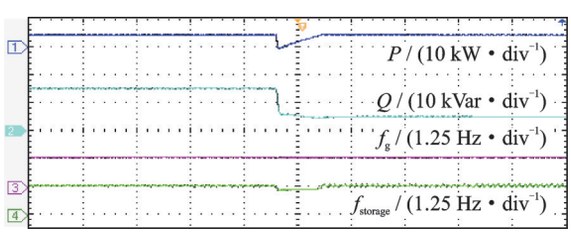

Fig.25 Experimental result when microgrid voltage step changes from 121 V to 99 V

5 Conclusions

A multi-source independent microgrid system is studied in this paper. The diesel generator is used as the main power source to maintain the stability of

the voltage and frequency of the microgrid, the energy storage unit adopts the VSG technology to support the microgrid together with the main power source, and photovoltaic and wind power systems work under the MPPT mode. Based on MATLAB/Simulink, the simulation model of multi-source microgrid system is built to verify the reliability of independent microgrid system and the supporting function of energy storage unit under different working modes. The response and support function of the energy storage unit to the voltage and frequency of the microgrid system is also verified by experiments.

References

[1] ZHU Wei, XU Wei, ZHOU Zhichao. The development status and its prospect of micro grid in China[J]. Electric Age, 2012(10): 42-43,46. (in Chinese)

[2] QU M, MARNAY C, ZHOU N. Microgrid policy review of selected major countries, regions, and organizations: LBNL-5782E[R]. Berkeley, USA: Lawrence Berkeley National Laboratory, 2012.

[3] SEBASTIAN R, QUESADA J. Distributed control system for frequency control in an isolated wind system[J]. Renewable Energy, 2006, 31(3): 285-305.

[4] FAKHAM H, DI L, FRANCOIS B. Power control design of a battery charger in a hybrid active PV generator for load-following applications[J]. IEEE Transactions on Industrial Electronics, 2011, 58(1): 85-94.

[5] HAO Liang, ZHU Jiajia, DING Bin, et al. Research progress of materials and technology for electrochemical energy storage[J]. Journal of Nanjing University of Aeronautics & Astronautics, 2015, 47(5): 650-658. (in Chinese)

[6] ZHAO Bo, ZHANG Xuesong, LI Peng, et al. Optimal design and application of energy storage system in Dongfushan island stand-alone microgrid[J]. Automation of Electric Power Systems, 2013, 37(1): 161-167. (in Chinese)

[7] CHATZIVASILIADIS S J, HATZIARGYRIOU N D, DIMEAS A L. Development of an agent based intelligent control system for microgrids[C]//Proceedings of Power and Energy Society General Meeting. Pittsburgh, USA:[s.n.], 2008.

[8] TAMAKI M, UEHARA S, TAKAGI K, et al. Demonstration results using Miyako island mega-solar demonstration research facility[C]// Proceedings of Transmission and Distribution Conference and Exposition (T&D). Orlando, USA:[s.n.], 2012.

[9] ZHAO Jie, WANG Shuo, SHEN Dali, et al. Control and simulation of a microgrid with different types of distributed generators[J]. Electric Power, 2013, 46(7): 105-110.(in Chinese)

[10] DENG Hao, CUI Shuangxi, SUN Yanping, et al. Study on modelling and simulation of the wind/PV/storage hybrid in islanding micro-grid system[J]. High Voltage Apparatus, 2019, 55(10): 141-147. (in Chinese)

[11] GUO Li, FU Xiaopeng, LI Xialin, et al. Coordinated control of battery storage and diesel generators in isolated AC microgrid systems[C]//Proceedings of the 7th International Power Electronics and Motion Control Conference. Harbin, China: IEEE, 2012.(in Chinese)

[12] HU J, CAO J, GUERRERO J M, et al. Improving frequency stability based on distributed control of multiple load aggregators[J]. IEEE Transactions on Smart Grid, 2017, 8(4): 1553-1567.

[13] BEVRANI H, ISE T, MIURA Y. Virtual synchronous generators: A survey and new perspectives[J]. International Journal of Electrical Power & Energy Systems, 2014, 54(1): 244-254.

[14] ZHANG Xing, ZHU Debin, XU Haizhen. Review of virtual synchronous generator technology in distributed generation[J]. Journal of Power Supply, 2012(3): 1-6,12. (in Chinese)

[15] ZHONG Q C, NGUYEN P L, MA Z, et al. Self-synchronized synchronverters: Inverters without a dedicated synchronization unit[J]. IEEE Transactions on Power Electronics, 2013, 29(2):617-630.

[16] HAO Zhenyang, XU Jian, WANG Xuerui, et al. A control method for three-phase PWM rectifier with function of friendly interaction between grid and load[J]. Journal of Nanjing University of Aeronautics & Astronautics, 2020, 52(2): 199-206.(in Chinese)

[17] ZHANG Yu, CAI Xu, ZHANG Chen, et al. Transient synchronization stability analysis of voltage source converters: A review[J]. Proceedings of the CSEE, 2021, 41(5): 1687-1702.

[18] LIU Qihui, LU Shengjian. Charging and discharging control strategy based on virtual synchronous machine for electrical vehicles participating in frequency regulation of microgrid[J]. Automation of Electric Power Systems, 2018, 42(9):171-179.(in Chinese)

Acknowledgement This research was supported by the

Science and Technology Research & Development Project of China Construction Second Engineering Bureau Ltd.(No. 91110000100024296D180009).

Authors Mr. **CHEN Xing** is a senior engineer. His main research interests are new energy technology application and water environmental protection technology application.

Prof. **CAO Xin** received the B.E., M.S., and Ph.D. degrees in electrical engineering from Nanjing University of Aeronautics and Astronautics(NUAA), Nanjing, China, in 2003, 2006 and 2010, respectively. He is currently a professor at College of Automation Engineering, NUAA. His current research focuses on distributed generation and renewable energy, switched reluctance machines, and high speed machines.

Author contributions Mr. **CHEN Xing** contributed to the background of the study and designed the study. Miss **QIAN Shengnan** complied the models and wrote the manuscript. Mr. **LI Fei** modified and improved the model. Mr. **GE Zhaohui** contributed to data for analysis. Prof. **CAO Xin** revised and modified the manuscript. All authors commented on the manuscript draft and approved the submission.

Competing interests The authors declare no competing interests.

(Production Editor:SUN Jing)

采用虚拟同步机技术的多源独立微网建模与实现

陈 星[1],钱胜南[2],李 飞[1],葛朝晖[1],曹 鑫[2]

(1.中建中环工程有限公司,南京 211100,中国;2.南京航空航天大学自动化学院,南京 211106,中国)

摘要:为提高孤立岛屿、偏远地区等电力设施建设薄弱地方的生活水平、用电经济性和环保性,研究了一种多源独立微网系统,包含柴油发电机、光伏发电系统、风力发电系统和储能单元。同时,为实现多源微网交流母线电压和频率的稳定控制,在储能单元中引入虚拟同步机技术,将储能电池的充放电控制模拟成为具有同步电机的控制行为特征,从而为多源微网提供阻尼和惯量支撑。分析了各子系统的运行方式和控制原理,给出了虚拟同步机的算法原理与储能单元的控制方法,以及不同环境条件下微网系统工作模式。基于MATLAB/Simulink搭建多源微网系统仿真模型,仿真结果表明:微网系统在不同工作模式下可稳定运行,采用虚拟同步机技术的储能单元可以为微网系统提供良好的电压和频率支撑。实验验证了储能单元对微网系统电压和频率的响应和支撑功能。

关键词:独立微网;风/光/柴储;虚拟同步机;建模